Catalysis Today 217 (2013) 80–85

Contents lists available at ScienceDirect

Catalysis Today

journal homepage: www.elsevier.com/locate/cattod

Review

Methylene dipyridine nanoparticles stabilized on Fe_3O_4 as catalysts for efficient, green, and one-pot synthesis of pyrazolophthalazinyl spirooxindoles

Seyed Mohsen Sadeghzadeh*, Mohammad Ali Nasseri

Department of Chemistry, College of Sciences, Birjand University, P.O. Box 97175-615, Birjand, Iran

ARTICLE INFO

Article history:
Received 7 April 2013
Received in revised form 20 July 2013
Accepted 29 July 2013
Available online 12 September 2013

Keywords:
Fe_3O_4\methylene dipyridine
Magnetic nanoparticles
Pyrazolophthalazinyl spirooxindoles
One-pot synthesis
Green chemistry

ABSTRACT

Surface functionalization of magnetic particles is an elegant way to bridge the gap between heterogeneous and homogeneous catalysis. The introduction of magnetic particles (MPs) in a variety of solid matrices allows the combination of well-known procedures for catalyst heterogenization with techniques for magnetic separation. We have conveniently loaded base groups on magnetic particles supports in which dipyridin-2-ylmethanol is used as aminating agent. The main targets are room temperature, solvent-free conditions, rapid (immediately) and easy immobilization technique, and low cost precursors for the preparation of highly active and stable MPs with high densities of functional groups. The inorganic, magnetic, solid base catalyst was characterized via Fourier transform infrared spectroscopy (FT-IR), X-ray diffraction (XRD), thermal gravimetric analysis (TGA), transmission electron microscopy (TEM) and vibrating sample magnetometer (VSM). The catalyst is active for the synthesis of pyrazolophthalazinyl spirooxindoles and the products are isolated in high to excellent yields (90–93%). Supporting this base catalyst on magnetic particles offers a simple and non-energy-intensive method for recovery and reuse of the catalyst by applying an external magnet. Isolated catalysts were reused for new rounds of reactions without significant loss of their catalytic activity.

Contents

---

* Corresponding author. Tel.: +98 561 2502065; fax: +98 561 2502065.
E-mail addresses: SM_Sadeghzadeh@yahoo.com, sadeghzadeh_sm@yahoo.com (S.M. Sadeghzadeh).

0920-5861/$ – see front matter © 2013 Elsevier B.V. All rights reserved.
http://dx.doi.org/10.1016/j.cattod.2013.07.018

1. Introduction

In recent years, core–shell multi-components have attracted intense attention because of their potential applications in catalysis [1]. Different from single-component that can only supply people with one function, the core–shell multi-components can integrate multiple functions into one system for specific applications [2–6]. Moreover, the interactions between different components can greatly improve the performance of the multi-components system and even generate new synergetic properties. Among the core–shell structured composites, the composites with magnetic core and functional shell structures have received especial attention because of their potential applications in catalysis, drug storage/release, selective separation, chromatography, and chemical or biologic sensors [7–12]. The magnetic core has good magnetic responsibility, and can be easily magnetized. Therefore, the composites with magnetic core can be conveniently collected, separated or fixed by external magnet [13]. Spiro compounds represent an important class of naturally occurring substances characterized by highly pronounced biological properties. The spirooxindole system is the core structure of many pharmacological agents and natural alkaloids [14–18].

Herein we report the fabrication of base group incorporated into a mesoporous hyperbranched propyltriethoxysilane shell that are coated on magnetic nanoparticles which catalyzed the synthesis Pyrazolophthalazinyl Spirooxindoles under solvent-free conditions at room temperature (Scheme 1).

2. Experimental

Chemical materials were purchased from Fluka and Merck in high purity. Melting points were determined in open capillaries using an Electrothermal 9100 apparatus and were uncorrected. Morphology was analyzed using transmission electron microscopy (TEM) on a JEOL-2010. Powder X-ray diffraction data were obtained using Bruker D8 Advance model with Cu Kα radition. Mass spectra were recorded on Shimadzu GCMS-QP5050 Mass Spectrometer. The magnetic measurement was carried out in a vibrating sample magnetometer (VSM – 4 inch, Daghigh Meghnatis Kashan Co., Kashan, Iran) at room temperature. NMR spectra were recorded in DMSO on a Bruker Advance DRX-400 MHz instrument spectrometer using TMS as internal standard. IR spectra were recorded on a Perkin Elmer 781. The purity determination of the products and reaction monitoring were accomplished by TLC on silica gel polygram SILG/UV 254 plates.

2.1. *General procedure for the preparation of Fe_3O_4 nanoparticles*

The synthesis procedure is illustrated as follows: (1) 0.01 mol $FeCl_2{\cdot}4H_2O$ and 0.03 mol $FeCl_3{\cdot}6H_2O$ were dissolved in to 200 mL distilled water, followed by the addition of PEG (1.0 g, MW 6000). (2) Sodium hydroxide (NaOH) was added to the solution and the pH value was controlled in the range $12 \leq pH \leq 13$. (3) Different amount of hydrazine hydrate ($N_2H_4{\cdot}H_2O$, 80% concentration) was added to the above suspension. The reaction was continued for about 24 h at room temperature. During this period, the pH value was adjusted by NaOH and kept in the range $12 \leq pH \leq 13$. The black Fe_3O_4 NPs were then rinsed several times with ionized water.

2.2. *General procedure for the preparation of $Fe_3O_4\backslash SiO_2$ nanoparticles*

0.02 mol of Fe_3O_4 MNPs were dispersed in a mixture of 80 mL of ethanol, 20 mL of deioned water and 2.0 mL of 28 wt% concentrated ammonia aqueous solution ($NH_3{\cdot}H_2O$), followed by the addition of 0.20 g of tetraethyl orthosilicate (TEOS). After vigorous stirring for 24 h, the final suspension was repeatedly washed, filtered for several times and dried at 60 °C in the air.

2.3. *General procedure for the preparation of $Fe_3O_4\backslash SiO_2\backslash$3-chloropropyltriethoxysilane nanoparticles*

2 mmol of $Fe_3O_4\backslash SiO_2$ MNPs and 20 mL THF were mixed together in a beaker, and then 20 mmol of NaH was dispersed in to the mixture by ultrasonication. 22 mmol 3-chloropropyltriethoxysilane was added drop-wise at room temperature and stirred for another 16 h at 60 °C. The resultant products were collected and washed with ethanol and deionized water in sequence, and then dried under vacuum at 60 °C for 2 h for further use.

2.4. *General procedure for the preparation of $Fe_3O_4\backslash SiO_2\backslash$propyltriethoxysilane\methylene dipyridine nanoparticles*

2 mmol of $Fe_3O_4\backslash SiO_2\backslash$3-chloropropyltriethoxysilane were dispersed in a mixture of 80 mL of ethanol, 20 mL of deioned water and 2.0 mL of 28 wt% concentrated ammonia aqueous solution ($NH_3{\cdot}H_2O$), followed by the addition of 20 mmol of compound dipyridin-2-ylmethanol. After vigorous stirring for 24 h, the final suspension was repeatedly washed, filtered for several times and dried at 60 °C in the air.

2.5. *General procedure for the synthesis of pyrazolophthalazinyl spirooxindoles*

A mixture of phthalic anhydride (1 mmol), isatin (1 mmol), malononitrile (1 mmol), hydrazine (1 mmol), and $Fe_3O_4\backslash$dipyridine MNPs (0.0008 g) was stirred at room temperature under solvent-free conditions for 50 min. Upon completion, the progress of the

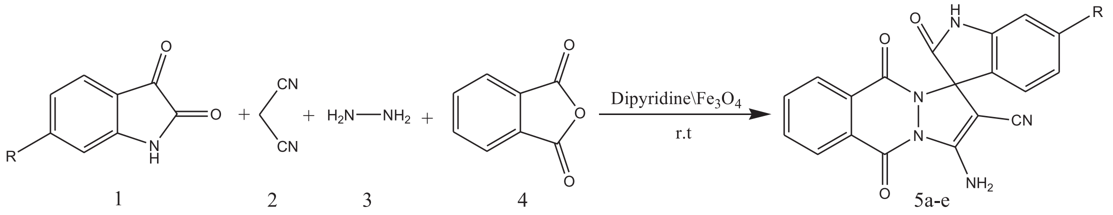

Scheme 1. Synthesis of pyrazolophthalazinyl spirooxindoles catalyzed by $Fe_3O_4\backslash$methylene dipyridine at room-temperature under solvent-free.

reaction was monitored by TLC when the reaction was completed, EtOH was added to the reaction mixture and the Fe_3O_4\methylene MNPs was separated by external magnet. Then the solvent was removed from solution under reduced pressure and the resulting product purified by recrystallization using ethanol.

2.6. Data for compounds

2.6.1. Compound (**5a**)

IR (KBr) υ cm^{-1}: 3439, 3350, 2209, 1756, 1678, 1653, 1465, 1364, 1257, 1163; ^1H NMR; δ, ppm: 10.92 (s, 1H, NH), 8.32 (s, 2H, NH_2), 8.30–8.32 (m, 1H, ArH), 7.98–8.06 (m, 3H, ArH), 7.30 (d, J = 7.0 Hz, 1H, ArH), 7.21 (t, J = 7.5 Hz, 1H, ArH), 6.88 (t, J = 7.5 Hz, 1H, ArH), 6.83 (d, J = 7.5 Hz, 1H, ArH); ^{13}C NMR; δ, ppm: 173.0, 156.8, 153.3, 152.5, 142.5, 135.8, 134.5, 131.3, 129.5, 128.6, 128.4, 127.3, 125.7, 125.5, 123.4, 114.7, 110.8, 70.5, 60.8.

2.6.2. Compound (**5b**)

IR (KBr) υ cm^{-1}: 3356, 3317, 2210, 1741, 1721, 1695, 1658, 1626, 1603, 1556, 1543, 1535, 1495, 1434, 1373, 1264, 1202, 1165, 1149, 820, 702; ^1H NMR; δ, ppm: 10.82 (s, 1H, NH), 8.33 (s, 2H, NH_2), 8.31 (d, J = 8.0 Hz, 1H, ArH), 8.06 (d, J = 7.5 Hz, 1H, ArH), 7.98–8.03 (m, 2H, ArH), 7.32 (s, 1H, ArH), 7.13 (d, J = 8.0 Hz, ArH), 6.82 (d, J = 8.0 Hz, 1H, ArH), 2.24 (s, 3H, CH_3); ^{13}C NMR; δ, ppm: 172.5, 156.5, 152.5, 151.3, 139.7, 135.2, 134.5, 131.6, 130.5, 128.6, 127.8, 127.5, 127.3, 125.4, 125.4, 114.1, 110.2, 69.7, 60.6, 20.8.

2.6.3. Compound (**5c**)

IR (KBr) υ cm^{-1}: 3361, 3250, 2210, 1768, 1708, 1665, 1646, 1620, 1553, 1475, 1411, 1363, 1257, 1167, 1134, 1115, 1029, 827, 698; ^1H NMR; δ, ppm: 11.09 (s, 1H, NH), 8.40 (s, 2H, NH_2), 8.31 (d, J = 8.0 Hz, 1H, ArH), 8.01–8.09 (m, 3H, ArH), 7.73 (d, J = 2.0 Hz, 1H, ArH), 7.40 (dd, J = 8.5, 2.0 Hz, 1H, ArH), 7.00 (d, J = 8.0 Hz, 1H, ArH); ^{13}C NMR; δ, ppm: 172.3, 156.3, 152.7, 151.8, 141.1, 135.2, 134.6, 130.3, 128.6, 127.5, 127.4, 127.3, 127.2, 126.4, 124.8, 114.5, 111.5, 69.7, 59.1.

2.6.4. Compound (**5d**)

IR (KBr) υ cm^{-1}: 3392, 3358, 2218, 1757, 1699, 1661, 1622, 1611, 1571, 1552, 1481, 1443, 1375, 1275, 1260, 1162, 1145, 1124, 812, 806, 700; ^1H NMR; δ, ppm: 11.09 (s, 1H, NH), 8.40 (s, 2H, NH_2), 8.32 (dd, J = 8.5, 2.0 Hz, ArH), 8.00–8.09 (m, 3H, ArH), 7.80 (d, J = 2.0 Hz, 1H, ArH), 7.48 (dd, J = 8.5, 2.0 Hz, 1H, ArH), 6.90 (d, J = 8.5 Hz, 1H, ArH); ^{13}C NMR; δ, ppm: 172.1, 156.4, 152.7, 152.0, 141.3, 135.1, 134.3, 133.2, 128.6, 127.5, 127.6, 127.5, 127.4, 127.1, 114.5, 114.4, 112.4, 69.6, 59.7.

2.6.5. Compound (**5e**)

IR (KBr) υ cm^{-1}: 3423, 3315, 1750, 1702, 1660, 1610, 1557, 1472, 1455, 1383, 1337, 1310, 1263, 1212, 1142, 1085, 1032, 840, 775, 701; ^1H NMR; δ, ppm: 11.50 (s, 1H, NH), 8.45 (s, 1H, ArH), 8.34 (d, J = 7.5 Hz, 1H, ArH), 8.19 (d, J = 8.0 Hz, 1H, ArH), 7.99–8.03 (m, 3H, ArH), 7.75 (br s, 2H, NH_2), 7.07 (d, J = 7.5 Hz, 1H, ArH).

3. Results and dscussion

We report the synthesis of a magnetic particle-based solid base with a high density of methylene dipyridine base groups and discuss its performance as a novel strong and stable solid base. W were intrigued by the possibility of applying dipyridin-2-ylmethanol and nanotechnology for the design of a novel, active, recyclable, and magnetically recoverable quinuclidin base derivative for the first time (Fig. 1).

3.1. XRD

The structural properties of synthesized Fe_3O_4\$SiO_2$\Methylene dipyridine MNP was analyzed by X-ray power diffraction (XRD). As shown in Fig. 2, XRD patterns of the synthesized Fe_3O_4\$SiO_2$\methylene dipyridine nanoparticle display several relatively strong reflection peaks in the 2θ region of 20°–70°, which is quite similar to those of Fe_3O_4 nanoparticles reported by other group. The discernible six diffraction peaks in Fig. 2a can be indexed to (2 2 0), (3 1 1), (4 0 0), (4 2 2), (5 1 1), and (4 4 0) which match well with the database of magnetite in JCPDS (JCPDS card No. 19-0629) file. Besides the peak of iron oxide, the XRD pattern of Fe_3O_4\$SiO_2$\methylene dipyridine core–shell nanoparticles presented a broad featureless XRD peak at low diffraction angle, which corresponded to the amorphous state SiO_2 shells (Fig. 2b) (JCPDS card No. 29-0085).

3.2. FT-IR

The successful synthesis of the Fe_3O_4\dipyridine nanoparticles were confirmed by the FTIR spectra. Peak appeared at 3100 cm^{-1}, 2930 cm^{-1}, 1090 cm^{-1}, and 590 cm^{-1} are due to the stretching of the C—H aromatic group, the C—H aliphatic group, O—Si group, and Fe—O group in the Fe_3O_4\dipyridine MNP (Fig. 2c).

3.3. Thermo-gravimetric analysis (TGA)

The thermal behavior of Fe_3O_4\SiO_2\methylene dipyridine MNPs is shown in Fig. 2d. This was evaluated to be 1.5% according to the TG analysis. The analysis showed two decreasing peaks. First

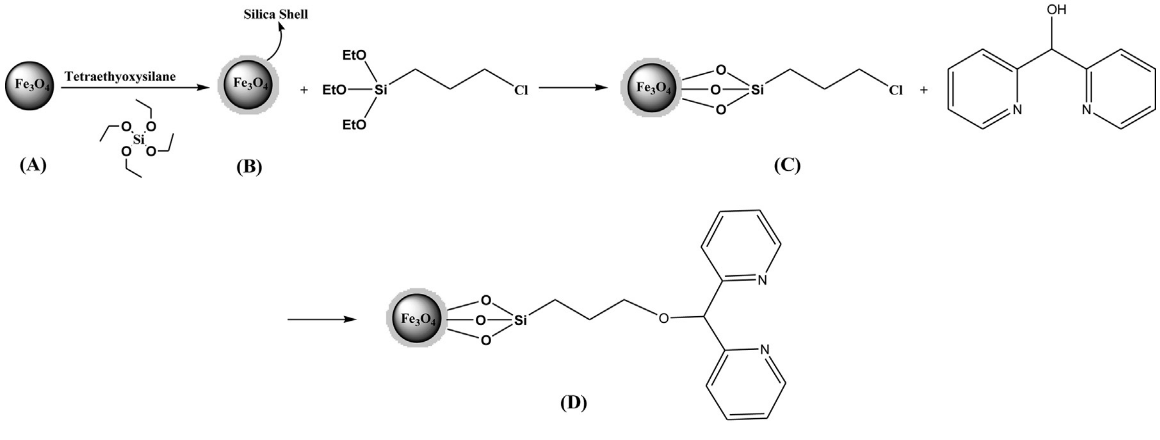

Fig. 1. Schematic illustration of the synthesis for Fe_3O_4\dipyridine.

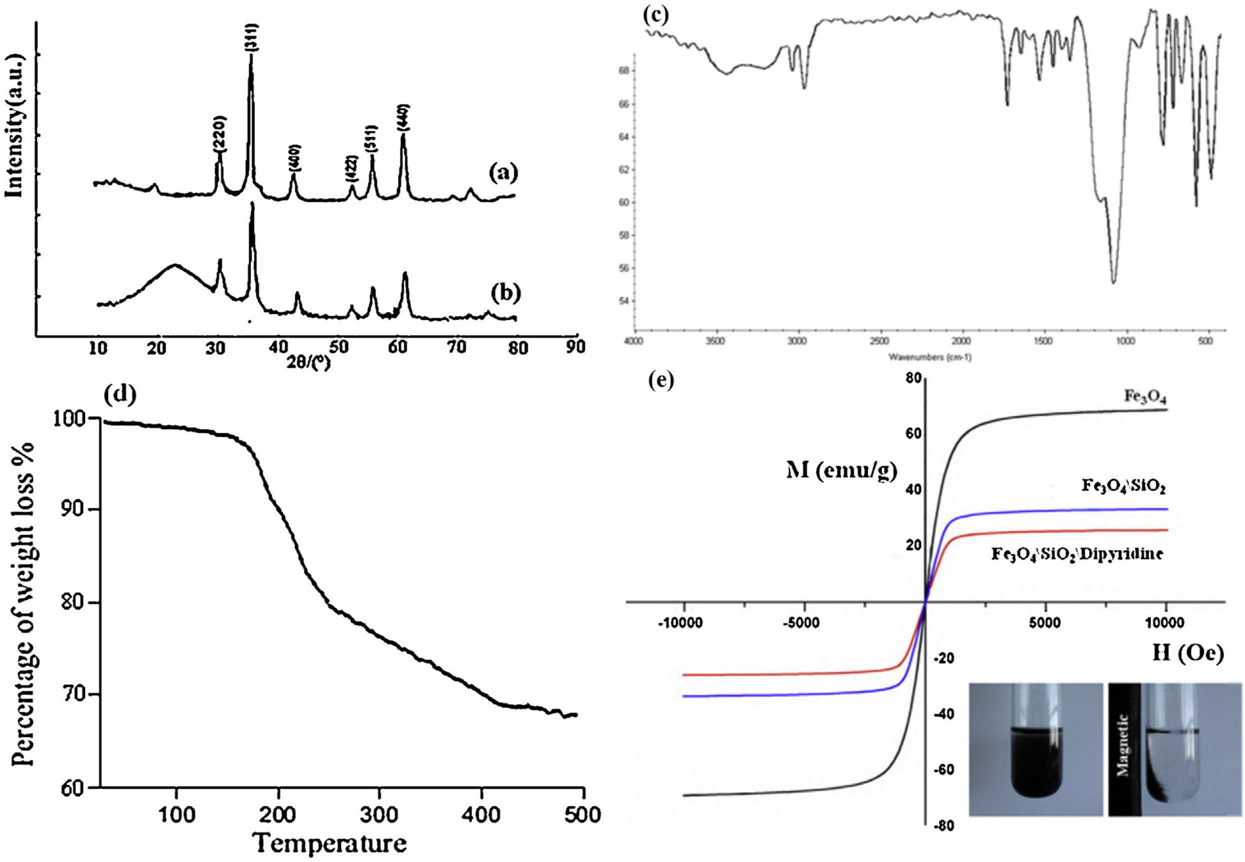

Fig. 2. XRD analysis of (a) Fe_3O_4, (b) $Fe_3O_4\backslash SiO_2\backslash$methylene dipyridine, (c) FTIR spectra of $Fe_3O_4\backslash$dipyridine, (d) TGA diagram of $Fe_3O_4\backslash SiO_2\backslash$methylene dipyridine MNPs, (e) room-temperature magnetization curves of the Fe_3O_4, $Fe_3O_4\backslash SiO_2$, and $Fe_3O_4\backslash SiO_2\backslash$dipyridine MNP.

peak appears at temperature around 130–150 °C due to desorption of water molecules from the catalyst surface. This is followed by a second peak at 425–450 °C, corresponding to the loss of the organic spacer group.

3.4. Magnetic properties of the $Fe_3O_4\backslash SiO_2\backslash$dipyridine MNP

Fig. 2e presented the magnetic hysteresis loops of the uncoated Fe_3O_4 powder (a), $Fe_3O_4\backslash SiO_2$ powder (b) and $Fe_3O_4\backslash SiO_2\backslash$Dipyridine powder (c) in an applied field of 10 kOe at 300 K. It is clearly seen from these magnetic hysteresis loops that all the samples have stronger magnetism with negligible coercivity and remanence at room temperature. Their saturation magnetization was 68.86, 33.40 and 25.84 emu/g, respectively. Compared with the uncoated Fe_3O_4 particles, the saturation magnetization of the $Fe_3O_4\backslash SiO_2$ MNP obviously decreased because the diamagnetic contribution of the thick SiO_2 resulted in a low mass fraction of the Fe_3O_4 magnetic substance. Nevertheless, there was only smaller difference of saturation magnetization between $Fe_3O_4\backslash SiO_2$ and $Fe_3O_4\backslash SiO_2\backslash$dipyridine. This is because thin outermost layer dipyridine shell cannot cause a larger mass fraction change of the Fe_3O_4 magnetic substance from $Fe_3O_4\backslash SiO_2$ to $Fe_3O_4\backslash SiO_2\backslash$dipyridine. Though the saturation magnetization of $Fe_3O_4\backslash SiO_2\backslash$dipyridine particles is less than the magnetite nanoparticles as magnetic core, it may be believed to possess enough strong magnetic attraction for effectively magnetic separation.

3.5. TEM

The size and structure of the $Fe_3O_4\backslash SiO_2\backslash$Methylene dipyridine MNPs were also evaluated using transmission electron microscopy (TEM) (Fig. 3). The average size of Fe_3O_4 MNP is about 10–15 nm

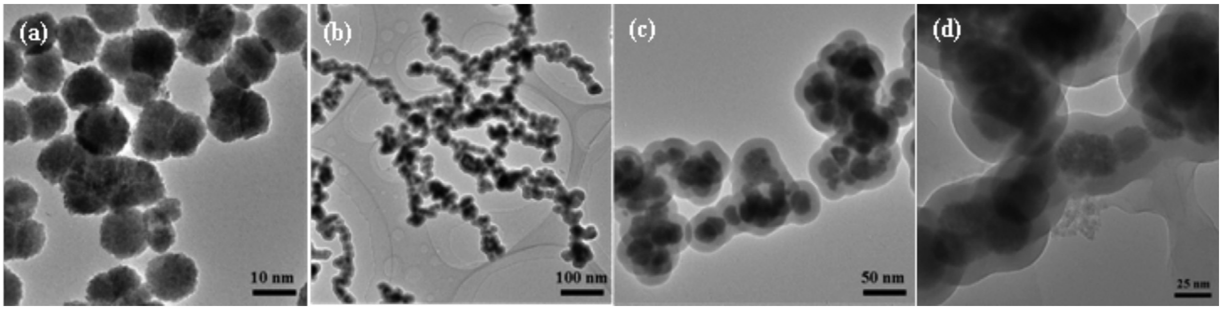

Fig. 3. (a) TEM image of Fe_3O_4 MNPs, (b) TEM image of $Fe_3O_4\backslash SiO_2$ MNPs, (c) TEM image of $Fe_3O_4\backslash SiO_2\backslash$methylene dipyridine MNPs, (d) $Fe_3O_4\backslash$dipyridine MNPs after reuse ten times. Agglomeration of $Fe_3O_4\backslash$dipyridine MNPs can be seen.

Table 1
Solvent screening for the reaction between phthalic anhydride, isatin, malononitrile, and hydrazine.[a]

Yield (%)[b]	Solvent	Entry
80	H_2O	1
73	EtOH	2
51	CH_3CN	3
32	THF	4
39	CH_2Cl_2	5
21	Toluene	6
73	EtOAC	7
trace	n-Hexane	8
trace	$CHCl_3$	9
trace	Dioxane	10
77	MeOH	11
65	DMSO	12
56	DMF	13
92	Solvent free	14

[a] Reaction conditions: phthalic anhydride (1 mmol), isatin (1 mmol), malononitrile (1 mmol), Hydrazine (1 mmol), and magnetic nanocatalyst (0.001 g) at room-temperature for 60 min.

[b] Isolated yields.

(Fig. 3a). After being coated with a SiO_2 layer, the typical core–shell structure of the $Fe_3O_4\backslash SiO_2$ MNPs can be observed. The dispersity of $Fe_3O_4\backslash SiO_2$ MNPs is also improved, and the average size increases to about 20–30 nm (Fig. 3b). The average size of $Fe_3O_4\backslash SiO_2\backslash$methylene dipyridine MNPs is about 35–50 nm, but the aggregation of the $Fe_3O_4\backslash SiO_2\backslash$methylene dipyridine is more evident than that of $Fe_3O_4\backslash SiO_2$ MNPs (Fig. 3c).

3.6. *Catalytic activity of $Fe_3O_4\backslash SiO_2\backslash$dipyridine MNPs for the one-pot synthesis of pyrazolophthalazinyl spirooxindoles*

We thought to optimize the reaction conditions, the same reaction was carried out in various solvents under similar conditions. In this study, it was found that solvent-free is a more efficient and superior solvent (Table 1, Entries 14) over other solvents (Table 1, Entries 1–13) with respect to reaction time and yield of the desired pyrazolophthalazinyl spirooxindoles.

At this stage, the amount of catalyst necessary to promote the reaction efficiently was examined. It was observed that the variation for $Fe_3O_4\backslash$dipyridine MNP had an effective influence. The best amount of $Fe_3O_4\backslash$dipyridine MNP is 0.0008 g which afforded the desired product in 92% yields (Fig. 4a).

Under the optimal conditions, the reaction progress in the presence of 0.0008 g of $Fe_3O_4\backslash$dipyridine MNPs was monitored by GC (Fig. 4b). Using this catalyst system, excellent yields of pyrazolophthalazinyl spirooxindoles can be achieved in 50 min. No apparent by-products were observed by GC in all the experiments and the cyclic carbonate was obtained cleanly in 92% yield.

It is important to note that the magnetic property of $Fe_3O_4\backslash$dipyridine MNPs facilitates its efficient recovery from the reaction mixture during work-up procedure. The activity of the recycled catalyst was also examined under the optimized conditions. After the completion of reaction, the catalyst was separated by an external magnet, washed with methanol and dried at the pump. The recovered catalyst was reused for ten consecutive cycles without any significant loss in catalytic activity (Fig. 4c).

Amount of leached catalysts after each catalytic cycle is shown in Fig. 5, which clearly demonstrates the practical recyclability and stability of this catalyst. The $Fe_3O_4\backslash$dipyridine MNP before use can be seen result in the change of the morphology and size of the obtained $Fe_3O_4\backslash$dipyridine MNP after reuse ten times (Fig. 3d).

In order to show the unique catalytic behavior of $Fe_3O_4\backslash$dipyridine MNPs in these reactions, we have performed one-pot reaction of phthalic anhydride, isatin, malononitrile, and hydrazine in the presence of a catalytic amount of $H_3PW_{12}O_{40}$,

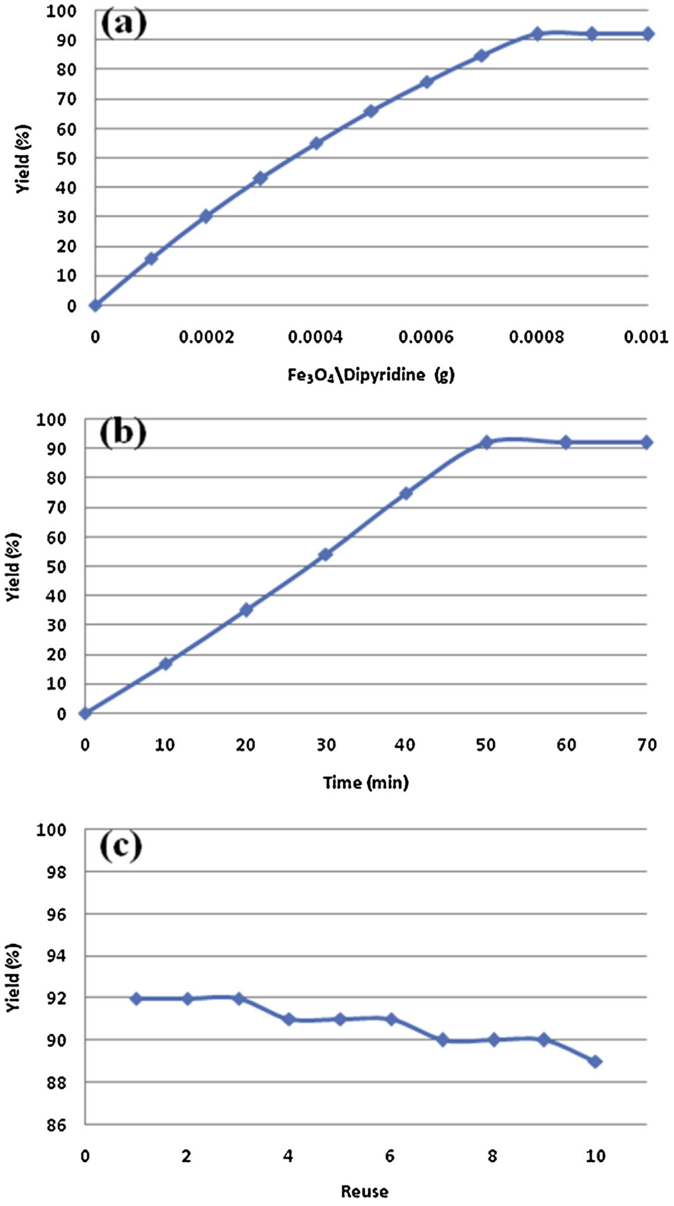

Fig. 4. (a) Effect of increasing amount of $Fe_3O_4\backslash$dipyridine MNPs on the preparation of pyrazolophthalazinyl spirooxindoles, (b) reaction progress monitored by GC, and (c) reuses performance of the catalysts.

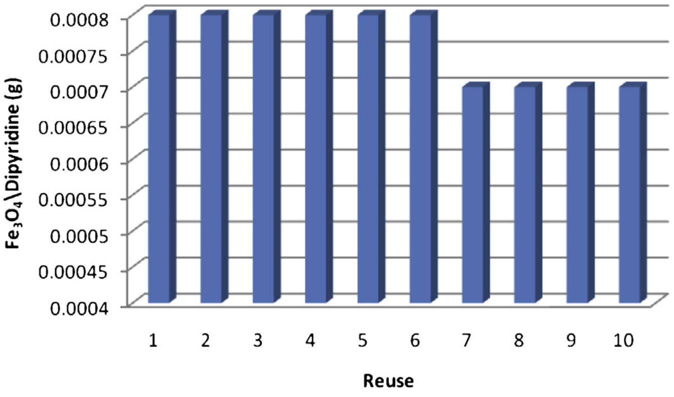

Fig. 5. Amount of leached catalysts after each catalytic cycle.

Table 2
Comparison of the catalytic efficiency of Fe_3O_4\dipyridine MNPs with some catalysts.

Entry	Catalyst	Time (h)	Yield (%)[a]
1	Fe_3O_4\dipyridine MNPs	1	92
2	$H_3PW_{12}O_{40}$	1	12
3	$NbCl_5$	1	trace
4	PEG-SO_3H	1	28
5	$InCl_3$	1	trace
6	$Pd(PPh_3)_4$	1	13
7	Cerium (IV) ammonium nitrate	1	trace

[a] Isolated yield, conditions: catalyst (0.0008 mmol), phthalic anhydride (1 mmol), isatin (1 mmol), malononitrile (1 mmol), hydrazine (1 mmol), room temperature, solvent-free.

Table 3
Synthesis of pyrazolophthalazinyl spirooxindoles using Fe_3O_4\dipyridine as catalyst.

Entry	R	Product	Time (min)	Yield (%)[a]	Mp (°C)
1	H	**5a**	50	92	266–269 [17]
2	Me	**5b**	50	90	279–281 [18]
3	Cl	**5c**	50	91	>300 [18]
4	Br	**5d**	50	92	>300 [18]
5	NO_2	**5e**	50	93	283–285 [17]

[a] Isolated yield.

$NbCl_5$, PEG-SO_3H, $InCl_3$, $Pd(PPh_3)_4$ and cerium(IV) ammonium nitrate (Table 2). As it is evident from Table 2, Fe_3O_4\dipyridine MNPs is the most effective catalyst for this purpose, leading to the formation of pyrazolophthalazinyl spirooxindoles in a good yield.

After optimization of the reaction conditions, to delineate this approach, particularly in regard to library construction, this methodology was evaluated by using variety of different substituted isatins in the presence of Fe_3O_4\dipyridine MNPs under similar conditions (Table 3). As expected, satisfactory results were observed, and the results are summarized in Table 3. As can be seen from Table 3, electronic effects and the nature of substituents on the isatins did not show strongly obvious effects in terms of yields under the reaction conditions. Isatins containing electron-withdrawing groups or electron-donating were employed and reacted well to give the desired products in excellent yields with high purity.

4. Conclusions

In conclusion, we have developed the current important areas of heterogenization of methylene dipyridine, which is a rapidly developing research area. The main objectives are room temperature, solvent-free conditions, a rapid (immediately) and easy immobilization technique, and low cost precursors for the preparation of highly active and stable MPs with high densities of functional groups. Furthermore, applying the young area of magnetic particles which are intrinsically not magnetic, but can readily be magnetized by an external magnet, can have a positive effect on high activity on one hand and separation and recycling on the other hand.

References

[1] C.L. Zhu, M.L. Zhang, Y.J. Qiao, G. Xiao, F. Zhang, J. Phys. Chem. C 114 (2010) 16229–16235.
[2] J.Q. Hu, Y. Bando, J.H. Zhan, D. Golberg, Appl. Phys. Lett. 85 (2004) 3593–3595.
[3] B. Liu, H.C. Zeng, Small 1 (2005) 566–571.
[4] J. Cao, J.Z. Sun, J. Hong, H.Y. Li, H.Z. Chen, M. Wang, Adv. Mater. 16 (2004) 84–87.
[5] X.M. Sun, Y.D. Li, Angew. Chem. Int. Ed. 43 (2004) 597–601.
[6] Q.B. Wang, Y. Liu, Y.G. Ke, H. Yan, Angew. Chem. Int. Ed. 47 (2008) 316–319.
[7] J.L. Lyon, D.A. Fleming, M.B. Stone, P. Schiffer, M.E. Williams, Nano Lett. 4 (2004) 719–723.
[8] P.P. Yang, Z.W. Quan, Z.Y. Hou, C.X. Li, X.J. Kang, Z.Y. Cheng, J. Lin, Biomaterials 30 (2009) 4786–4795.
[9] M. Zhang, Y.P. Wu, X.Z. Feng, X.W. He, L.X. Chen, Y.K. Zhang, J. Mater. Chem. 20 (2010) 5835.
[10] S.S. Liu, H.M. Chen, X.H. Lu, C.H. Deng, X.M. Zhang, P.Y. Yang, Angew. Chem. Int. Ed. 49 (2010) 7557–7561.
[11] Y.H. Won, D. Aboagye, H.S. Jang, A. Jitianu, L.A. Stanciu, J. Mater. Chem. 20 (2010) 5030–5034.
[12] Y. Li, J.S. Wu, D.W. Qi, X.Q. Xu, C.H. Deng, P.Y. Yang, X.M. Zhuang, Chem. Commun. (2008) 564–566.
[13] (a) J. Deng, L.P. Mo, F.Y. Zhao, L.L. Hou, L. Yang, Z.H. Zhang, Green Chem. 13 (2011) 2576–2584;
(b) R.B.N. Baig, R.S. Varma, Chem. Commun. 49 (2013) 752–770;
(c) J. Deng, L.P. Mo, F.Y. Zhao, Z.H. Zhang, S.X. Liu, ACS Comb. Sci. 14 (2012) 335–341;
(d) F.P. Ma, P.H. Li, B.L. Li, L.P. Mo, N. Liu, H.J. Kang, Y.N. Liu, Z.H. Zhang, Appl. Catal. A: Gen. 457 (2013) 34–41;
(e) R.B.N. Baig, R.S. Varma, Green Chem. 15 (2013) 398–417.
[14] T.H. Kang, K. Matsumoto, Y. Murakami, H. Takayama, M. Kitajima, N. Aimi, H. Watanabe, Eur. J. Pharmacol. 444 (2002) 39–45.
[15] J. Ma, S.M. Hecht, Chem. Commun. 10 (2004) 1190–1191.
[16] T. Usui, M. Kondoh, C.B. Cui, T. Mayumi, H. Osada, Biochem. J. 333 (1998) 543–548.
[17] G. Shanthi, P.T. Perumal, J. Chem. Sci. 122 (2010) 415–421.
[18] X.N. Zhang, Y.X. Li, Z.H. Zhang, Tetrahedron 67 (2011) 7426–7430.